The TAU isoform 1N4R restores vulnerability of *MAPT* knockout human iPSC-derived neurons to Amyloid beta-induced neuronal dysfunction

Buchholz S[1,2], Bell-Simons M[1,2], Al Kabbani MA[1,2], Kluge L[1,2], Cagmak C[1,2], Klimek J[1,2] and Zempel H[1,2*]

[1]Institute of Human Genetics, Faculty of Medicine and University Hospital Cologne, University of Cologne, 50931 Cologne, Germany

[2]Center for Molecular Medicine Cologne (CMMC), Faculty of Medicine and University Hospital Cologne, University of Cologne, 50931 Cologne, Germany

[*]Correspondence to: hans.zempel@uk-koeln.de

Short title: 1N4R TAU isoform mediates Abeta toxicity in human neurons

+++SUPPLEMENTAL MATERIAL+++

A

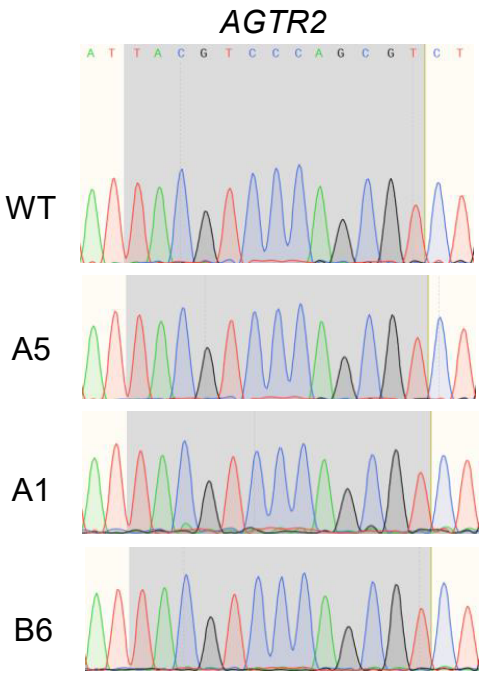

B

Gene	Seq. match	Clone 1 (A5)	Clone 2 (A1)	Clone 3 (B6)
ASTE1	65%	wt/wt	wt/wt	wt/wt
SLC19A	65%	wt/wt	wt/wt	wt/wt
AGTR2	65%	wt/wt	wt/wt	wt/wt
SNRPA1	65%	wt/wt	wt/wt	wt/wt
NDOR1	75%	wt/wt	wt/wt	wt/wt
TMEM218	75%	wt/wt	wt/wt	wt/wt
CCDC102A	70%	wt/wt	wt/wt	wt/wt
CEP131	75%	wt/wt	wt/wt	wt/wt

C

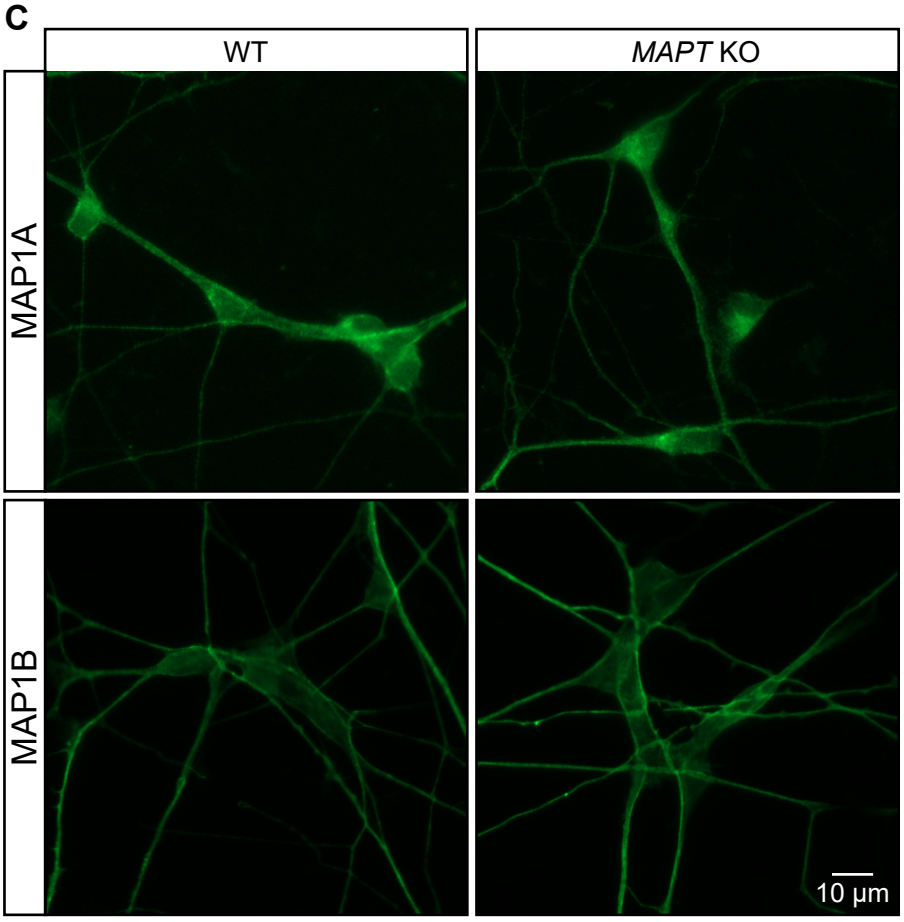

D

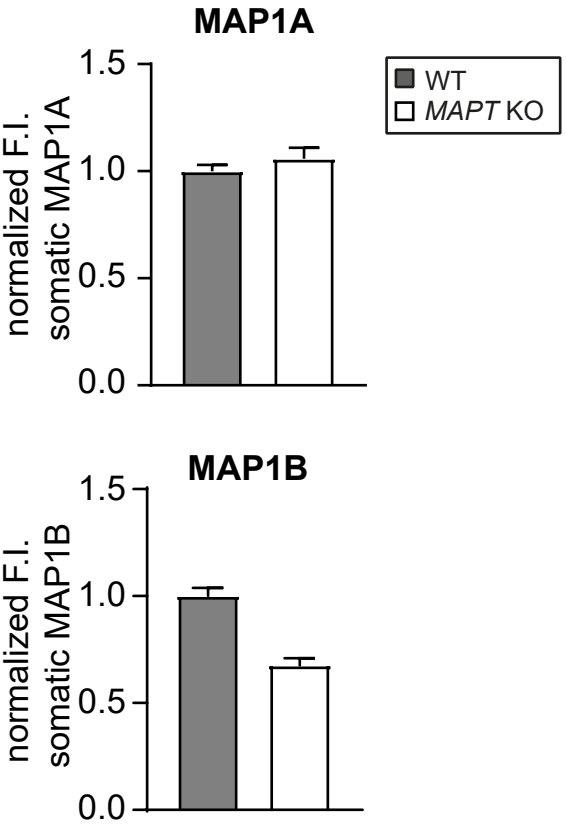

Figure S1: No detectable Cas9 off-target activity and no compensatory upregulation of MAP1A/B in TAU KO iNeurons. **A)** Exemplary sequencing results of predicted gRNA off-target AGTR2. All three TAU KO clones harbour the WT sequence. **B)** Overview of sequenced gRNA off-targets for all three TAU KO clones. All sequences match the reference (WT) sequence, indicating no off-target effects of the Cas9 nuclease. **C)** Immunofluorescence images of WT (left panels) and TAU KO (right panels) iNeurons at d21, stained for microtubule-associated proteins 1 (MAP1) A and B. **D)** Quantification of fluorescence intensity of MAP1A and MAP1B in the soma of WT and TAU KO iNeurons. Error bars represent SEM.

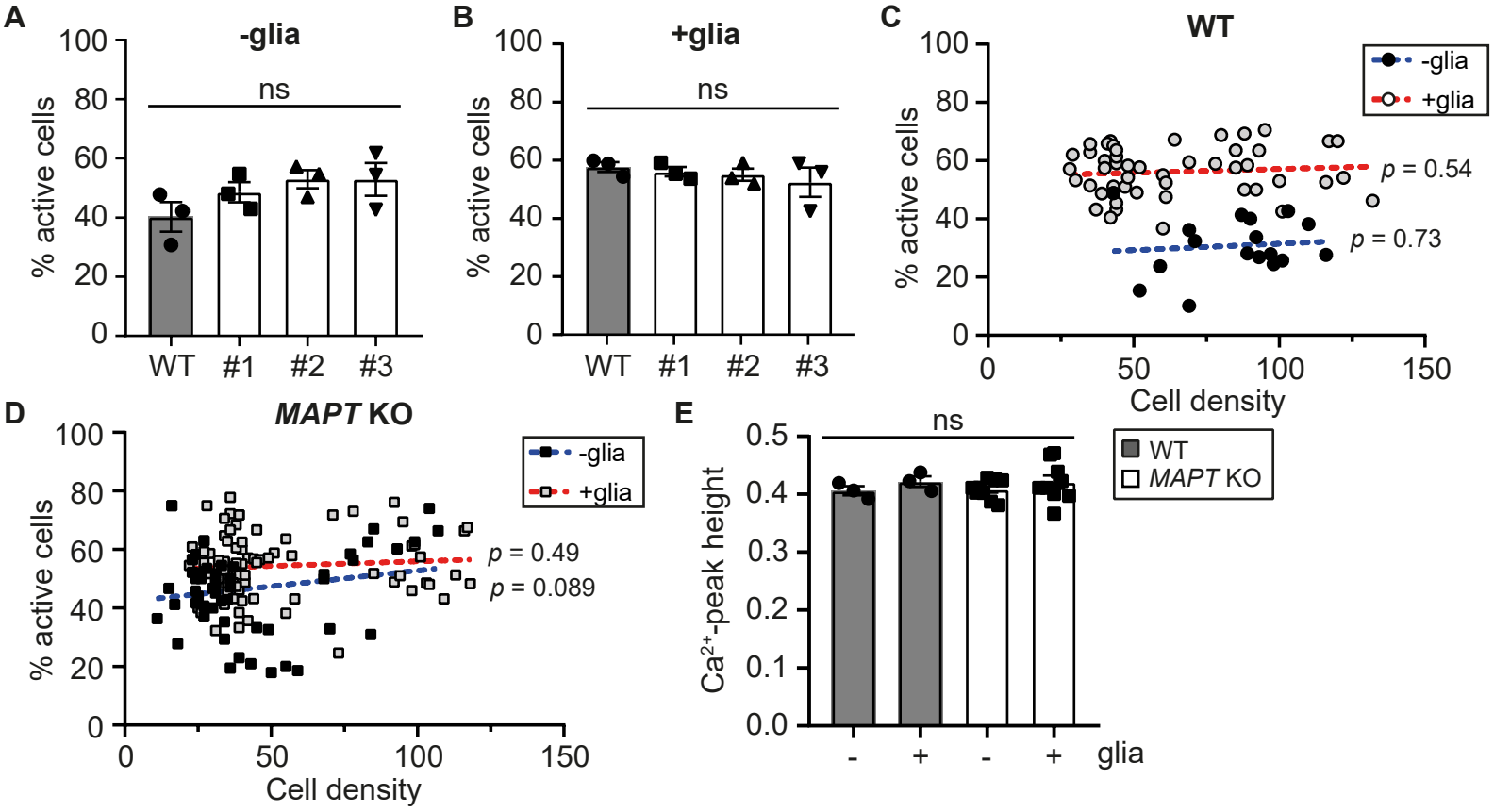

Figure S2: Neuronal activity is independent of cellular density and is consistent within TAU KO clones.
A) Comparison of neuronal activity of WT iNeurons and the three generated TAU KO clones (d14) in the absence of primary astrocytes. Error bars represent SEM; Shapiro-Wilk test was performed to test for normal distribution, afterwards, statistical analysis was performed by one-way ANOVA with correction for multiple comparisons (Tukey's test). Ns= not significant. **B)** Comparison of neuronal activity of WT iNeurons and the three generated TAU KO clones (d14) in the presence of primary astrocytes. Error bars represent SEM; Shapiro-Wilk test was performed to test for normal distribution, afterwards, statistical analysis was performed by one-way ANOVA with correction for multiple comparisons (Tukey's test). Ns= not significant. **C)** Correlation plot of the percentage of active cells in WT neuronal cultures in dependence of cellular density. Dashed lines indicate the corresponding linear regression model and do not show a significant correlation between cellular density and neuronal activity. **D)** Correlation plot of the percentage of active cells in TAU KO neuronal cultures in dependence on cellular density. Dashed lines indicate the corresponding linear regression model and do not show a significant correlation between cellular density and neuronal activity. **E)** Calcium peak height was quantified using an automated workflow and compared between both genotypes, WT and TAU KO, in dependence on co-cultures with primary astrocytes. Error bars represent SEM; Shapiro-Wilk test was performed to test for normal distribution, afterwards, statistical analysis was performed by one-way ANOVA with correction for multiple comparisons (Tukey's test). Ns= not significant.

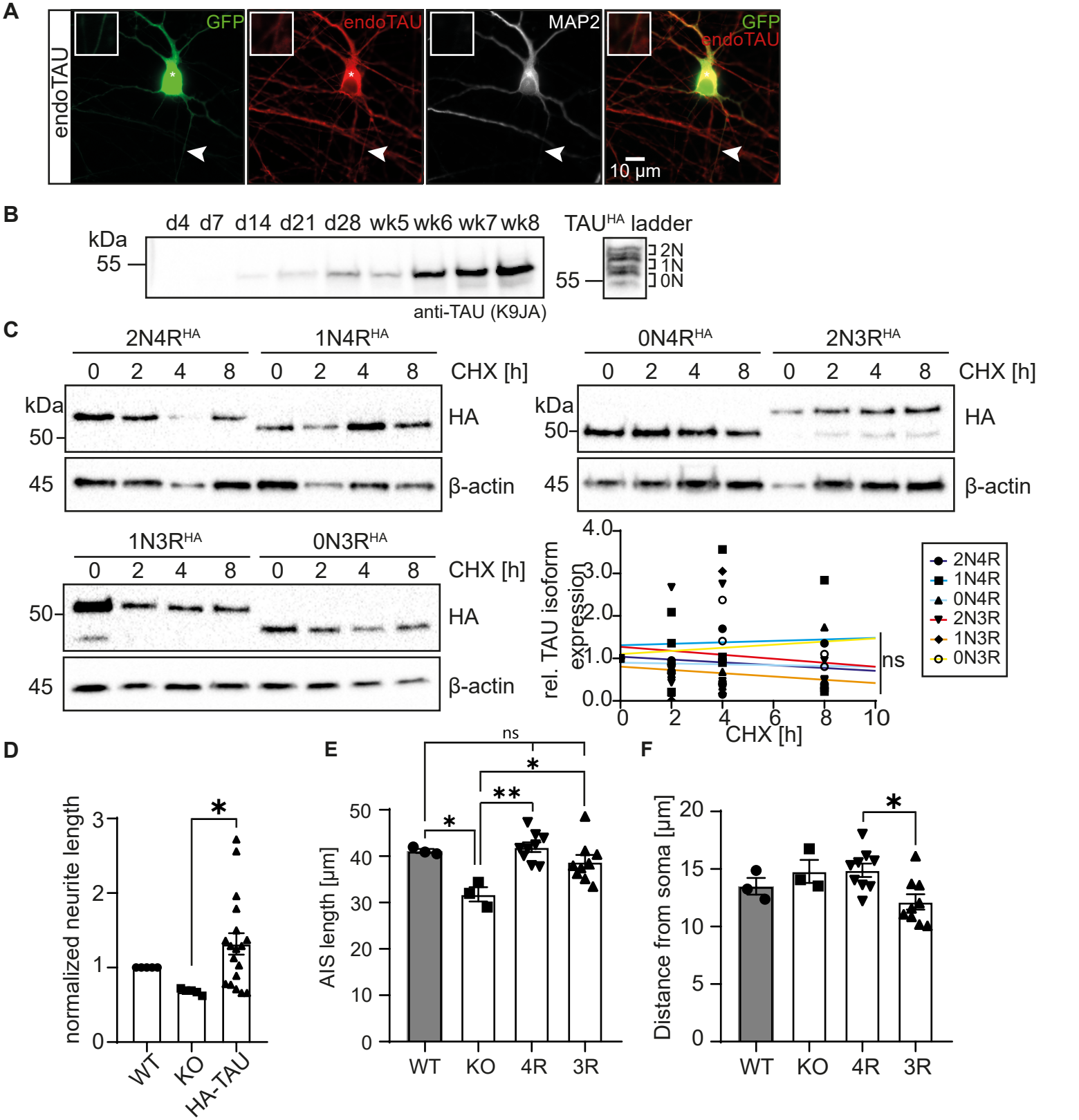

Figure S3: Only the shortest TAU isoforms are expressed in WT iNeurons and TAU isoforms do not differ in their stability. **A)** TAU isoform expression of WT iNeurons was assessed by Western blot analysis (left side) after the indicated time points of neuronal differentiation. In addition, all six human TAU isoforms (HA-tagged) were expressed in HEK293 cells (right side) to compare the sizes of endogenous TAU with the TAU ladder. Note that the HA-tag (size ~1.1 kDa) leads to a shift in isoform size compared to un-tagged endogenous TAU. The experiment was performed independently for three times. **C)** Quantification of axonal enrichment of endogenous TAU in WT iNeurons (d21) expressing GFP as a volume marker. N=3, n=20, error bars represent SEM. **D)** A cycloheximide (CHX) chase was performed to analyze TAU isoform stability in HEK293 cells. Cells were transfected with individual TAU isoforms, and protein translation was inhibited using CHX for 0, 2, 4, and 8 hours, 24 hours after transfection. Graph (lower right panel) shows the average linear regression of the isoform stability over time out of three independent experiments and reveals no significant differences between the isoforms. **E)** Comparison of neurite length between WT, TAU KO and TAU KO iNeurons re-expressing HA-tagged TAU. Error bars represent SEM; Shapiro-Wilk test was performed to test for normal distribution, afterwards, statistical analysis was performed by one-way ANOVA with correction for multiple comparisons (Tukey's test). N=4, n=20. Statistical significance: * $p \leq 0.05$, ** $p \leq 0.01$, *** $p \leq 0.001$, ns = not significant. **F)** Comparison of AIS length and **G)** distance from soma between WT, TAU KO, and TAU KO iNeurons re-expressing either 3R or 4R-TAU isoforms. Error bars represent SEM; Shapiro-Wilk test was performed to test for normal distribution, afterwards, statistical analysis was performed by one-way ANOVA with correction for multiple comparisons (Tukey-'s test). N=3, n=20. Statistical significance: * $p \leq 0.05$, ** $p \leq 0.01$, *** $p \leq 0.001$, ns = not significant.

Table S1 gRNA sequences and *MAPT* sequencing primer used in this study.

gRNA oligos/seq. primer	Sequence 5' -> 3'
gRNA1_oligo1	CACCGTCACGCTGGGACGTACGGGT
gRNA1_oligo2	AAACACCCGTACGTCCCAGCGTGAC
gRNA2_oligo1	CACCGCCGCCAGGAGTTCGAAGTGA
gRNA2_oligo2	AAACTCACTTCGAACTCCTGGCGGC
MAPT_E1_seq_fw	GGCCAACTGTTAGAGAGGGT
MAPT_E1_seq_rv	ACCGTGTCTGGCCATTATCT

Table S2 Off-target sequencing primer used in this study.

Target	Sequence 5' -> 3'
ASTE1_fw	GGAGAAAGCAGAGGAGGACC
ASTE1_rv	GGACCTTGCACAGACAGTTG
SLC19A_fw	GTGCTGGCCTTGGTATGTG
SLC19A_rv	GATTCTCTCCCCAGCTCTCC
AGTR2_fw	AGGTTGTGAAAGCTGATGAACA
AGTR2_rv	ACCTTCAAAATTCAGGCTGCA
SNRPA1_fw	ACTCCGAAACACACCCTAGG
SNRPA1_rv	TAATGAAGTCACCCGTGCCT
NDOR1_fw	GACCCTGACCAGCTCTTCAT
NDOR1_rv	TGAGGTCCAACAGGTAGTCG
TMEM218_fw	ATCTCTGGAGTCCTGGCTTC
TMEM218_rv	ACACACAGCCCACCACAT
CCDC102A_fw	CCTGAACCAAGAAAGCCGAG
CCDC102A_rv	ACTTAACCCCTTCCTTCCCG
CEP131_fw	TTACGGGACAAGTACGAGGC
CEP131_rv	CACCTCCTCCAGCTCCAG

Table S3 qRT-PCR primer used in this study.

qRT-PCR primer	Sequence 5' -> 3'
tTAU_fw	GTCGAAGATTGGGTCCCTGG
tTAU_rv	GACACCACTGGCGACTTGTA
HPRT_fw	GCTATTGTAATGACCAGTCAACAGGGGAC
HPRT_rv	CCTTGACCATCTTTGGATTATACTGCC

Table S4 Antibodies used in this study.

Antibody	Company	Cat. no.	Application	Dilution
Primary Antibodies				
Mouse monoclonal anti-Sox-2 (E-4)	Santa Cruz	sc-365823	ICC	1:100
Mouse anti-Oct3/4 (C-10)	Santa Cruz	sc-5279	ICC	1:100
Rabbit polyclonal anti-TAU (K9JA)	Dako	A0024	WB/ ICC	1:1000
Mouse monoclonal anti-HA (16B12)	Biolegend	90501	ICC	1:1000
Mouse monoclonal anti-TAU (A-5)	Santa Cruz	sc-390476	WB	1:500
Chicken polyclonal anti-MAP2	Abcam	ab5392	ICC	1:2000
Mouse monoclonal anti-GAPDH (1D4)	Novus Biologicals	NB300-221	WB	1:2000
Rabbit polyclonal anti-Trim46	Synaptic Systems	377003	ICC	1:500
HRP-conjugated mouse monoclonal anti-Beta Actin	Proteintech	HRP-60008	WB	1:10.000
Rabbit polyclonal anti-MAP1A	Sigma-Aldrich	HPA022275	ICC	1:200
Rabbit polyclonal anti-MAP1B	Sigma-Aldrich	HPA066488	ICC	1:200
Secondary Antibodies				
Donkey anti-mouse IgG AlexaFluor-488	Thermofisher Scientific	A21202	ICC	1:1000
Goat anti-chicken IgG AlexaFluor-647	Thermofisher Scientific	A21449	ICC	1:1000
Donkey anti-rabbit IgG AlexaFluor-488	Thermofisher Scientific	A21206	ICC	1:1000
Goat Anti-Mouse IgG (H+L), HRP-linked	Dianova	115-035-003	WB	1:10.000
Goat anti-rabbit IgG, HRP-linked	Cell Signaling Technologies	7074	WB	1:10.0000